

Surface, Thermal and Mechanical Characteristics of Polymeric Solids

Tisato Kajiyama, Noriaki Satomi, Keiji Tanaka and Atsushi Takahara

Department of Materials Physics & Chemistry,
Graduate School of Engineering, Kyushu University, 6-10-1 Hakozaki,
Higashi-ku, Fukuoka 812-8581, Japan

SUMMARY: Surface molecular motions of amorphous polymeric solids have been directly measured on the basis of lateral force microscopic (LFM) and scanning viscoelasticity microscopic (SVM) measurements. SVM measurement revealed that the molecular motion at the surface of the monodisperse polystyrene (PS) film with M_n less than ca.30k was fairly activated compared with that in a bulk region, mainly due to the surface segregation of chain end groups. Temperature dependent LFM and SVM measurement revealed that the surface glass transition temperature, T_g of the monodisperse PS film was lower than the bulk one, even though M_n was fairly large as 140k and also, that the time-temperature superposition was applicable to the surface relaxation process. The chain end group segregation at the air/PS interface was verified from the dynamic secondary ion mass spectroscopic (DSIMS) depth profiling of the proton and deuterium ion for the end-labeled deuterated-PS (dPS) film. These results suggest that the surface T_g is depressed due to an increase in free volume near surface region, being induced by the preferential surface localization of chain end groups.

Introduction

Recently, thermal molecular motion of polymer chains at the surface region has been paid great attention since this property is quite important for the practical applications as well as scientific interests.^{1,2)} Particular example is the glass transition behavior of polymer thin films. Since the polymer thin film has a large surface to volume ratio, the influence of surface on the glass transition temperature, T_g might be prominent. In the case of ultrathin polymer films, spectroscopic ellipsometry,³⁾ X-ray reflectivity,⁴⁾ positron annihilation lifetime spectroscopy,⁵⁾ and Brillouin light scattering⁶⁾ studies have indicated that T_g itself may be a function of film thickness and also, depends on whether the film is free-standing or in contact with a substrate, that is the extent of polymer/substrate

interaction. However, little study has been done on the glass transition behavior at free surfaces of bulk polymeric solids. The molecular dynamics simulation of atactic polypropylene on graphite predicted the decrease in density at the air/solid interface region.⁷⁾ Meyers and co-workers cast the question “Is the surface of polystyrene really glassy?”.⁸⁾ They used atomic force microscope (AFM) to study the wear of a PS surface and concluded from the recovery characteristics of the scratched pattern formed by a cantilever tip of AFM that the outermost surface of the PS film with molecular weight less than 24k was in a rubbery state. This experiment was performed under large deformation corresponding to a non-linear viscoelastic condition. However, no direct experimental evidence has been obtained for molecular motion in a linear viscoelastic response at the surface region.

The purpose of this study is to propose novel methods for the characterization of surface glass transition behavior for thick polymer films. The molecular weight dependence of surface molecular motions of the monodisperse polystyrenes (PS's) was studied on the basis of scanning viscoelasticity microscopy (SVM). The surface relaxation process of the monodisperse PS films was also studied based on the temperature dependent lateral force microscopy (LFM) and SVM measurements. In order to discuss the origin of activated surface molecular motion, the dynamic secondary ion mass spectroscopic (DSIMS) depth profiling was done for the end-labeled deuterated-PS(dPS).

Scanning Viscoelastic Microscopic Studies of Surface Molecular Motion for Monodisperse Polystyrene Films with Different Molecular Weights

Scanning force microscopy (SFM) is one of the family of scanning probe microscopy and has proven to be important for investigation of the surface morphology of materials with high resolution.⁹⁾ SFM images are created on the basis of the various forces acting between cantilever tip and sample surface such as van der Waals, electrostatic, frictional, magnetic forces and so on. AFM topographic image is obtained by detecting the normal force acting between sample surface and probe tip.¹⁰⁾ The magnitude of modulus for the generally used silicon or silicon nitride probe tip is 200-300 GPa, which is much higher than that of the polymer surface. Therefore, when the AFM observation is carried out in a

repulsive region of the force curve, the sample surface can be deformed due to the indentation of the tip. The modulation of the tip indentation leads to the modulation of the force acting between sample surface and probe tip. Figure 1 shows the schematic representation of the tip-surface interaction for SVM. If the modulation of the tip indentation is applied sinusoidally to the sample surface (stimulation strain), the dynamic viscoelastic properties at the sample surface can be evaluated by measuring the amplitude of the modulated response stress signal and the phase lag between modulation signal (stimulation strain) and modulated deformation signal (response stress).^{11,12)} A forced modulation AFM equipment, so-called “scanning viscoelasticity microscope (SVM)”, was designed by remodeling a commercially available AFM.^{13,14)} The purpose of this section is to investigate the surface thermal molecular motion of the monodisperse PS films on the basis of SVM measurement.

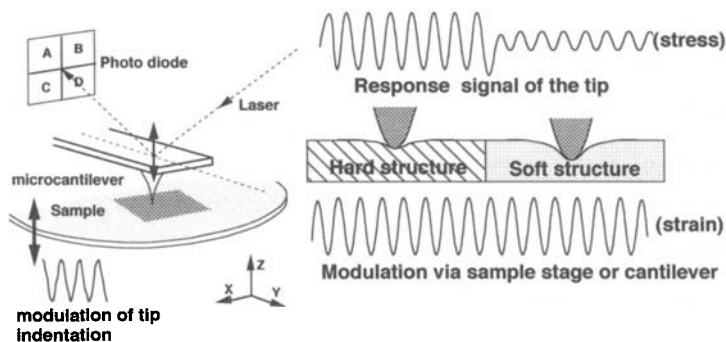


Figure 1 Schematic representation of tip-surface interaction for SVM.

Monodisperse PSs were prepared by a living anionic polymerization at 293 K using sec-butyllithium as an initiator. The magnitudes of M_n and M_w/M_n were determined via gel permeation chromatography (GPC) with polystyrene standards. The bulk T_g was evaluated on the basis of differential scanning calorimetric (DSC) measurement at a heating rate of $10 \text{ K} \cdot \text{min}^{-1}$ under dry nitrogen purge. The monodisperse PS films of ca. 200 nm thick were coated from a toluene solution onto a silicon wafer with native oxide layer by a spin-coating method. The surface dynamic viscoelastic functions of the monodisperse PS films were evaluated on the basis of SVM measurement, which was performed at 293 K in air under a repulsive force of ca. 10-25 nN. A commercially available silicon

nitride (Si_3N_4) cantilever with integrated tips was used. The nominal bending spring constant of the cantilever was $0.09 \text{ N}\cdot\text{m}^{-1}$. The modulation frequency and the modulation amplitude at the supporting part of the cantilever were 4 kHz and 1.0 nm, respectively. The SFM apparatus, SPA 300 (Seiko Instruments Industry Co., Ltd.) with an SPI 3700 controller was used for surface viscoelasticity measurement at air atmosphere.

¹³⁻¹⁵⁾ The cantilever tip is mounted on the piezoelectric bimorph. The cantilever position in the z-direction is modulated sinusoidally by applying an a.c. electric field to the piezoelectric bimorph transducer. The modulated force is detected by the deflection of the cantilever. The deflection signal obtained with position sensitive detector (PSD) is filtered by a band-pass filter (BPF) in order to remove the high- and low-frequency noises and feeds into a two-phase lock-in amplifier. The reference signal used is the sinusoidal signal from frequency generator which corresponds to the dynamic strain signal.

Figure 2 shows the M_n dependence of surface dynamic storage modulus, E' and surface $\tan \delta$ for the monodisperse PS films as well as the bulk $\tan \delta$ and bulk T_g values.^{14,15)} The magnitude of E' was calibrated by using a PS film with M_n of 1.8M. Since the concentration of chain end group is extremely low at the air surface in the case of the PS film with M_n of 1.8M, it seems reasonable to assume that thermal molecular motion at the film surface is comparable to that for the bulk sample even if the chain end groups are preferentially segregated at the film surface. Therefore, the magnitude of surface E' was calibrated on the assumption that the surface E' is equal to the bulk E' in the case of PS film with M_n of 1.8M. In a M_n range higher than 40.4k, the magnitudes of surface E' and surface $\tan \delta$ were independent of M_n and their magnitudes were ca. 4.5 GPa and 0.01, respectively, as shown in Figure 2. This indicates that the surface is in a glassy state at 293 K for the monodisperse PS film with larger M_n than 40.4k, judging from the magnitudes of surface E' and surface $\tan \delta$. Also, in the case of M_n smaller than 26.6k, the magnitudes of surface E' and surface $\tan \delta$ decreased and increased with a decrease in M_n , respectively. The magnitudes of surface E' and surface $\tan \delta$ indicate that the surface of the monodisperse PS films with M_n lower than 26.6k is in a glass-rubber transition or rubbery state even at 293 K. The bulk dynamic viscoelastic properties of

the monodisperse bulk PS samples were measured in order to compare with the surface one. In the case of M_n smaller than 26.6k, the magnitude of surface $\tan \delta$ was much higher than that of bulk $\tan \delta$ as shown in Figure 2. Thus, it can be reasonably concluded that the activation of surface molecular motion is more remarkable in the case of M_n less than 26.6k. These results clearly indicate that the surface T_g of the monodisperse PS film is more strongly dependent on M_n than the bulk T_g , because the chain end effect on surface T_g and surface $\tan \delta$ is more apparent than that on bulk $\tan \delta$.

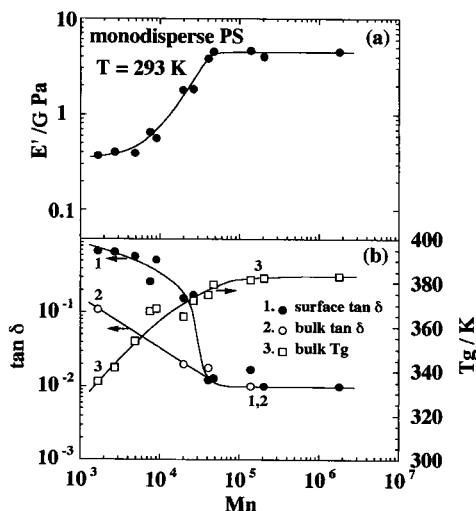


Figure 2 Molecular weight dependence of surface E' , surface $\tan \delta$, bulk $\tan \delta$, bulk T_g for the monodisperse PS films at 293 K.

Temperature Dependence of Surface Molecular Motion by Using Lateral Force Microscopy

LFM is a useful tool for the scanning rate and temperature dependent two-dimensional measurements of lateral force, which is evaluated by detecting the torsion of the sliding cantilever.⁹⁾ Since the force measured by LFM is the sum of frictional and adhesion forces acting between sample surface and cantilever tip, the term of LFM is used instead of "frictional force microscope" in this paper. The frictional behavior of polymeric solids is closely related to their dynamic viscoelastic properties,¹⁶⁾ so that it is possible to investigate surface molecular motions of the polymeric solids by using LFM which can detect lateral force between solid surface and sliding cantilever tip on nanometer scale.¹⁵⁾

In consideration that the scanning rate dependence of lateral force corresponds to the frequency dependence of loss modulus, E'' , it is apparent that no distinct scanning rate dependence of lateral force is observed in the cases of the glassy surface or rubbery one. Whereas, in the case of the surface in a glass-rubber transition state, the maximum peak of frictional force with the scanning rate is generally observed due to an appearance of the E'' maximum in a transition region. Therefore, when the magnitude of lateral force evaluated by LFM exhibits an apparent scanning rate dependence, it can be concluded that the surface is in a glass-rubber transition state. Since our LFM apparatus can not cover a whole scanning rate range corresponding to the glass-rubber transition at only a certain measuring temperature such as room temperature, the scanning rate dependence of lateral force was evaluated at various temperatures in order to apply the time-temperature superposition principle.

LFM used for temperature dependent studies is SPA300HV (SII, Co., Ltd.) with SPI3800 controller. The scanning stage of LFM was heated to a certain measuring temperature under vacuum. Piezoscanner was thermally insulated from the heating stage. Temperature dependent LFM measurements were carried out in vacuo in order to avoid surface oxidation and a capillary force effect induced by surface-adsorbed water. The magnitude of lateral force was evaluated by a line scan mode.

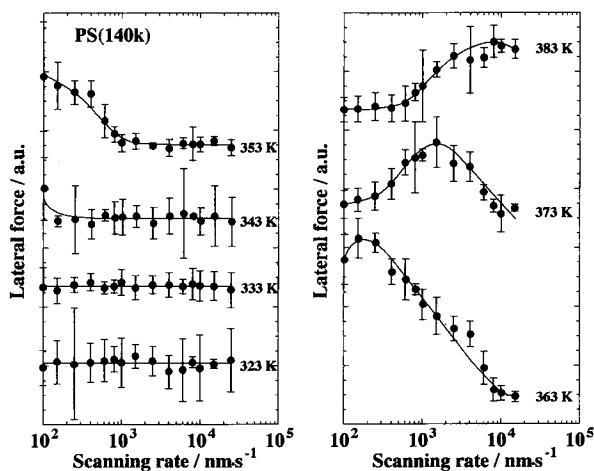


Figure 3 Scanning rate dependence of lateral force with various temperatures for the monodisperse PS film with M_n of 140k.

Figure 3 shows the scanning rate dependence of lateral force as a function of temperature for the monodisperse PS film with Mn of 140k. In the temperature range from 293 K to 333 K, no scanning rate dependence of lateral force was observed. This apparently indicates that the surface Tg of the monodisperse PS with Mn of 140k is higher than 333 K. In the temperature range from 343 K to 353 K, the magnitude of lateral force increased with a decrease in the scanning rate, especially at a lower scanning rate region. The scanning rate, at which the magnitude of lateral force starts to increase with a decrease in the scanning rate, was shifted to the higher scanning rate region with an increase in measuring temperature from 343 K to 353 K. The existence of the scanning rate dependence of lateral force indicates that the surface is in a glass-rubber transition state at a lower scanning rate region. Since the bulk Tg of PS with Mn of 140k evaluated by DSC was 382 K, it seems reasonable to conclude that the surface Tg was depressed compared with the bulk one, even though the molecular weight of the monodisperse PS is fairly high as 140k. Also, in the temperature range from 363 K to 383 K, the peak was clearly observed on the scanning rate-lateral force curve. At 383 K above the bulk Tg, the magnitude of lateral force decreased with a decrease in the scanning rate in a wide scanning rate region. This means that the PS surface is almost in a rubbery state. The shape of each curve in Figure 3 suggests that the master curve can be obtained by the horizontal and vertical shifts. Since the magnitude of lateral force showed a large scattering of data, only the magnitude of horizontal shift, a_T was evaluated.

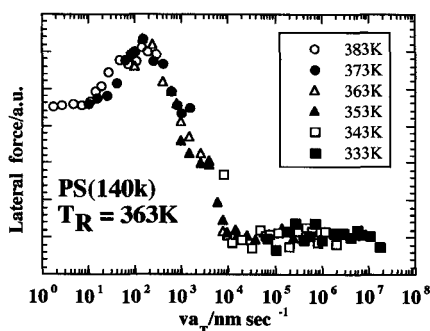


Figure 4 A master curve of the scanning rate-lateral force relationship for the monodisperse PS film with Mn of 140k drawn from the each curve in Figure 3. A reference temperature was 363K.

Figure 4 shows the master curve drawn by horizontal and vertical shifts of each curve shown in Figure 3 as a reference temperature of 363K. Since the master curve obtained corresponds to the scanning rate dependence of lateral force being expanded along the scanning rate axis, it seems reasonable to consider that the scanning rate dependence of lateral force exhibits a peak in a glass-rubber. Figure 4 clearly indicates that the time-temperature superposition, which is characteristic to the bulk viscoelastic properties of polymeric materials, can be applied to the surface relaxation process.

Figure 5 shows the relationship between a_T and reciprocal of measuring absolute temperature that followed the the Arrhenius equation. The magnitude of activation energy for the surface α -relaxation process calculated from the slope of the $\log a_T$ vs. $1/T$ plot was $220 \text{ kJ}\cdot\text{mol}^{-1}$. This magnitude is a little smaller than that for the bulk one of $360\text{-}430 \text{ kJ}\cdot\text{mol}^{-1}$.¹⁸⁾ At the air-polymer interface, an excess free volume is induced by the surface localization of the chain end groups as discussed below and also, the polymeric segment density at the air interface is less than that in the bulk based on simulation study.⁷⁾ Then, it can be predicted from the magnitude of activation energy that the energy barrier and/or the size of thermal molecular motion for the α -relaxation process at the air-polymer interface might be reduced in comparison with those for the bulk one, due to thermal segmental motion of PS chain into an air free space.

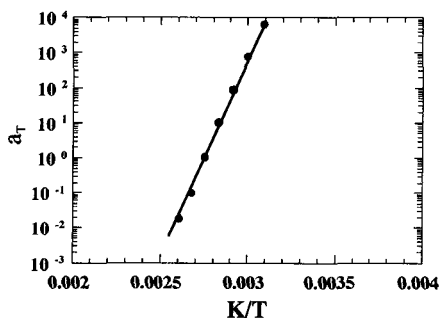


Figure 5 The relationship between a_T and reciprocal of measuring absolute temperature.

Temperature Dependent Scanning Viscoelasticity Microscopic (SVM) Measurements

Temperature dependent SVM measurement was carried out in vacuo by using the same SFM equipment as described above. Since the contact area between cantilever tip and PS surface depends on the magnitude of surface modulus in the case of the constant force operation, the actual stress was not evaluated at the present study.¹⁹⁾ The phase lag between stress and strain signals at the surface region was evaluated by SVM measurement at the frequency of 4 kHz. The magnitude of phase lag does not depend on the contact area between tip and the polymer surface. The force between cantilever tip and surface was controlled less than ca. 1nN in order to avoid the indentation of the tip at the temperature of the glass-transition region. The amplitude of apparent cantilever vibration was ca. 1nm. The monodisperse PS films with Mn of 4.9k, 53k, and 90k were prepared by spin-coating from a toluene solution at 2000rpm.

Figure 6 shows the temperature dependence of the phase lag between observed stress and strain signals for the monodisperse PS films with Mns of 4.9k, 53k, and 90k. The plots of $\tan\delta$ vs temperature for the bulk PS at 3.5Hz measured by Rheovibron are also plotted in the Figure 6. Even though the observed phase lag contains the contribution of the phase lag of the mechanical vibration system,⁹⁾ the calibration has not been done because the calibration constant including the phase lag of the system should be temperature-dependent. The magnitude of the phase lag started to increase at lower temperature than that of bulk $\tan\delta$ as shown in Figure 6. The onset of an increase in the phase lag, shown by the arrows in Figure 6 can be empirically defined as the surface Tg. The depression of the surface Tg for the PS films with Mns of 4.9k, 53k, 90k were ca. 110, 85, 65 K in comparison with the bulk Tg, respectively. Temperature dependent SVM of the PS film revealed that the surface molecular motion of PS was fairly activated even the case of Mn of 90k.

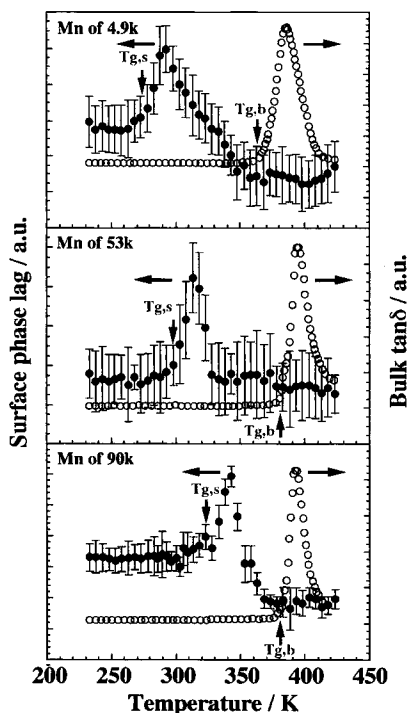


Figure 6 Temperature dependence of the phase lag between observed stress and strain signals for the monodisperse PS films with Mns of 4.9k, 53k and 90k. Surface and bulk Tg's are shown in the plots.

Depth Profile of Chain End Groups by Dynamic Secondary Ion Mass Spectroscopy

A depression in Tg at the film surface compared with that for the bulk sample has been explained by the surface localization of chain end groups.^{20,21)} However, the relationship between surface localization of chain end groups and activation of surface molecular motion has not been experimentally confirmed. The dPS of which chain end groups were labeled by protonated groups was prepared by a living anionic polymerization. The depth profiling of H⁺, D⁺ and C⁺ of the dPS film was carried out by using DSIMS measurement in order to confirm the surface localization of chain end groups. A platinum layer of 10 nm thick was sputter-coated on the surface of the end-labeled dPS film in order to avoid a charging up of the specimen during the DSIMS measurement.

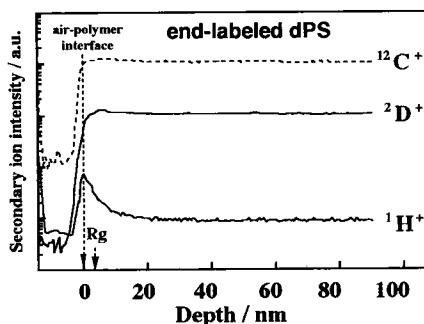


Figure 7 DSIMS depth profile of the end-labeled dPS film.

Figure 7 shows the typical DSIMS depth profile of the end-labeled dPS film. The dashed vertical line corresponds to the air/polymer interface. The steady-state etching proceeded during the etching process. The intensity of carbon ion, C^+ was almost constant at any depth position from the polymer film surface. Although, in general, the secondary ion efficiency of hydrogen atom is higher than that of heavy hydrogen atom, the stronger intensity of deuterium ion, D^+ than that of proton, H^+ was maintained during the etching of the polymer film. This stronger intensity of D^+ results from the larger fraction of heavy hydrogen atom in the end-labelled dPS. Figure 7 revealed an apparent increase in the intensity of H^+ and a decrease in that of D^+ in the air/polymer interface region. Since styrene unit was deuterated and protons were present only in both chain end portions, the DSIMS depth profile shows an apparent enrichment of chain end groups at the air/polymer interface. Since the surface localization of chain end groups induces the excess free volume fraction at the film surface compared with that in the bulk phase, the surface T_g becomes lower than the bulk T_g , resulting in that surface molecular motion at the film surface is fairly active in comparison with that for the bulk sample at room temperature, 293 K. The localization decay length of chain end groups was defined as the range from the air/polymer interface to the depth that the initial slope of H^+ profile crossed the bulk intensity. The localization decay length of chain end groups was about 4.4 nm and its value was almost comparable to the radius of gyration of an unperturbed chain, R_g of 3.3 nm.

Conclusions

Activation of thermal molecular motion at the surface of amorphous polymeric solids has been confirmed by SFM. SVM was revealed that the monodisperse PS film surface with M_n less than 26.6k was in a glass-rubber transition state or in a rubbery state even at 293 K due to the surface segregation of chain end groups. On the other hand, temperature dependent LFM and SVM measurement revealed that the surface molecular motion of PS was activated compared with the bulk one even though M_n of the monodisperse PS was so high as ca.100k. The chain end group segregation at the surface was verified from the DSIMS depth profiling of end-labeled dPS film. These results suggest that surface T_g is depressed due to an increase in free volume near surface region, induced by the preferential surface localization of chain end groups.

Acknowledgements. This work was partially supported by Grant-in-Aid for COE Research from Ministry of Education, Science, Sports and Culture, Japan.

References

1. M. Schrader and G. Loeb Eds. "*Modern Approaches to Wettability: Theory and Applications*", Plenum Press, New York, 1992
2. F. Garbassi, M. Morra and E. Occhiello, "*Polymer Surfaces from Physics to Technology*," John Wiley & Sons, New York, 1994
3. J. L. Keddie, R. A. L. Jones and R. A. Coury, *Europhys. Lett.*, **27**, 49(1994)
4. J. H. van Zanten, W. E. Wallace, and W. L. Wu, *Phys. Rev. E.*, **53**, R2053(1996)
5. De Maggio, W. E. Frieze, D. W. Gidley, M. Zhu, H. A. Hristov and A. F. Yee, *Phys. Rev. Lett.*, **78**, 1524(1997)
6. A. Forrest, K. Dalnoski-Veress, J. R. Stevens and J. R. Dutcher, *Phys. Rev. Lett.*, **77**, 2002(1996)
7. F. Mansfield, and D. N. Theodorou, *Macromolecules*, **24**, 6283(1991)
8. F. Meyers, B. M. DeKoven and J. T. Seitz, *Langmuir*, **8**, 2330 (1992)
9. J. Colton, A. Engel, J. E. Frommer, H. E. Gaub, A. A. Gewirth, R. Guckenberger, J. Rabe, W. M. Heckl, and B. Parkinson Eds, "*Procedures in Scanning Probe Microscopy*", John Wiley, NY, 1998.

10. G. Binnig, C. F. Quate, and C. G. Gerber, *Phys. Rev. Lett.* **56**, 930(1986)
11. P. Maivald, H. J. Butt, S. A. C. Gould, C. B. Prater, B. Drake, J. A. Gurley, V. B. Elings, and P. K. Hansma, *Nanotechnology* , **2**, 103(1991)
12. M. Radmacher, R. W. Tillmann, and H. E. Gaub, *Biophys. J.* , **64**, 735 (1993)
13. T. Kajiyama, K. Tanaka, I. Ohki, S.-R. Ge, J.-S. Yoon and A. Takahara, *Macromolecules*, **27**, 7932(1994)
14. K. Tanaka, A. Taura, S.-R. Ge, A. Takahara and T. Kajiyama, *Macromolecules*, **29**, 3040(1996)
15. T. Kajiyama, K. Tanaka and A. Takahara, *Macromolecules*, **30**, 280(1997)
16. K. A. Grosch, *Proc. R. Soc. London A* **274**, 21(1963)
17. T. Kajiyama, N. Satomi, K. Tanaka and A. Takahara, *Macromolecules*, **31** (1998)
18. N. G. McCrum, B. E. Read, G. Williams, “*Anelastic and Dielectric Effects in Polymeric Solids*”, John Wiley, London, 1967
19. H. Hertz, *J. Reine Angew. Math.* **92**, 156(1882)
20. A. M. Mayes, *Macromolecules*, **27**, 3114(1994).
21. T. Kajiyama, K. Tanaka and A. Takahara, *Macromolecules*, **28**, 3482(1995)